TELKOMNIKA, Vol. 11, No. 8, August 2013, pp. 4190~4199
e-ISSN: 2087-278X

Voltage and Reactive Power Control of Front-end Speed Controlled Wind Turbine via H_∞ Strategy

Haiying Dong*[1], Shuaibing Li[1], Lixin Cao[2], Hongwei Li[1]
[1]School of Automation & Electrical Engineering, Lanzhou Jiao Tong University, Anning West Road, 730070 Lanzhou, China, +86-0931-4956106/4956028
[2]Lanzhou Electric Corporation, No.66, Minle Road, 730050, Lanzhou, China, +86-0931-2866951-8010
Corresponding author, e-mail: hydong@mail.lzjtu.cn[1], lishuaibing1105@163.com

Abstract

*According to the characteristics like rapidity, time variability and the uncertainty of the input mechanical torque of front-end speed control wind turbine (*FSCWT*) with directly grid-connected and electrically excited synchronous generator (EESG), a double-loop H_∞ control approach was proposed. In which, a simpilified structure of brushless excitation system was used. For the inner loop, first H_∞ excitation controller was designed for realizing a fast excitation control; the second H_∞ power system stabilizer (PSS) was designed by solving the Riccati equation for the purpose of eliminating the oscillation and desynchronization of generator may caused by fast excitation to improve the system transient stability, which ensured the generator with a stable operation in grid-connecting and effectively solved the contradiction between fast excitation and transient stability. Then the designed H_∞ controllers were applied to the voltage and reactive power control system (VRCS), which realized the output voltage and reactive power control requriements by tuning the weighting functions. Simulation results show that the double-loop H_∞ control approach was more effective than the single H_∞ excitation control in voltage and reactive power control of FSCWT.*

Keywords*: voltage and reactive power control, H_∞ control, transient stability, front-end speed controlled wind turbine (FSCWT), electrically excited generaor (EESG).*

1. Introduction

The voltage and reactive power control of generators is of important significance to improve the stability of the power system, keep the voltage balance and minimize the transmission loss. As the proportion of grid-connected wind energy capacity in power system increased year by year, the grid-connecting of large-scale wind farms directly affect the power system stability. The wind generator output voltage and reactive power would be varied when a small signal disturbance or oscillations occured in power system. The voltage and reactive power control is necessary in order to keep a stable output voltage to maintain the power system voltage balance.

Scholars have made investigations on voltage and reactive power control of doubly fed Induction wind generators and direct-drive permanent magnet synchronous wind generators [1-3]. However, these types of generators are all of poor performence in low voltage ride through (LVRT) and reactive power surpport capability compared with FSCWT proposed in this paper as presented in Figure 1, which used a hydro-dynamic controlled gearbox instead of the electrical inverter and directly connected to grid with a rated voltage of 10KV without using transformer [4].

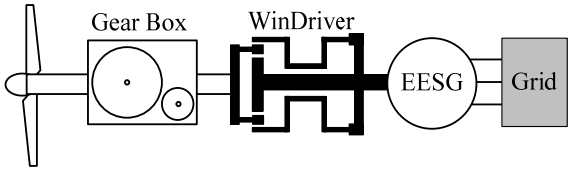

Figure 1. Structure of FSCWT

Received February 17, 2013; Revised March 25, 2013; Accepted May 16, 2013

For FSCWT, the output voltage and reactive power can be regulated by excitation control. In [5], a fast excitation control structure was presented and a H_∞ controller for output voltage real-time feedback control was designed accordingly, in which the influence of fast excitation control on the transient stability of synchronous generator was not considered; in [6-7], an exciter was proposed for electrically excited synchronous wind generaor by using optimal module and symmetrical optimal design techniques, which didn't take the effect of power system failure on voltage and reactive power into consideration. In this paper, a VRCS model was set up according to the fast excitation system and a H_∞ excitation controller was designed accordingly; on the bases of which, an equivalent simple machine infinite bus (SMIB) system was refined and a H_∞ PSS was designed in order to guarantee the transient stability.

2. Modelling of System

The unbalance of reactive power would cause a voltage deviation of power system from the set value, which reasults in an unstable operation of wind generators. It is the wind variation, the power system fault and the electrical equipment switching that lead to a reactive power change. For the purpose of meeting the reaquirements of voltage and reactive power control, an voltage and reactive power double loop control system was designed which structure can be seen in Figure 2. The speed deviation was used as input for H_∞ PSS in the outer loop, the reference value was compared with the feedback voltage of generator and the output of PSS, then the error was used as iuput for inner H_∞ excitation controller. So, the generator voltage can be regulated by controlling the output of PWM rectifier so that the generator voltage would maintain at a constant value.

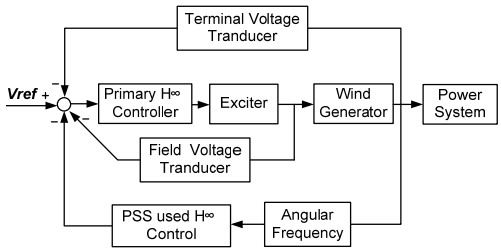

Figure 2. Voltage and Reactive Power Control Structure

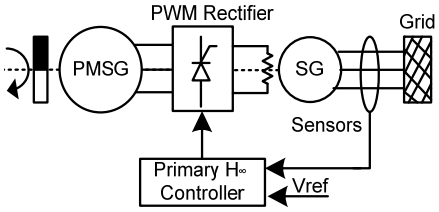

Figure 3. Structure of Excitation System

The IEEE AC5A recomend excitation system is a brushless excitation system consisted of a main exciter, a vice exciter and synchronous generator [8]. The field current was indirectly control by regulating excitation current of the main exciter, which caused an uncertainty and time-lag of the excitation control. The excitation system of EESG used in this paper was a simplified one [9] as is shown in Figure 3, which is made up by a permanent magnet synchronous generator and a full-controllable PWM rectifier.The voltage and reactive power can be adjusted by regulating the output voltage of rectifier.

Consider a general plant of the synchronous generator which can be represented in Park's framework by [10]:

$$\begin{cases} v_d = -R_s i_d - d/dt \cdot \psi_d + \omega_e \psi_q \\ v_q = -R_s i_q + d/dt \cdot \psi_q + \omega_e \psi_d \\ v_f = d/dt \cdot \psi_f + R_f i_f \\ 0 = d/dt \cdot \psi_D + R_D i_D \\ 0 = d/dt \cdot \psi_Q + R_Q i_Q \end{cases} \quad (1)$$

Where i_d and i_q are respectively the direct and transverse currents, i_D and i_Q are the direct and transverse damper's currents and i_f is the exciter current. ψ_d and ψ_q are the stator total

flux, ψ_f is the main field total flux. ψ_D and ψ_Q are the direct and transverse damper's total flux. R_s, R_f are respectively the stator resistance and the main field resistance, R_D and R_Q are the damper's resistances. ω_e is the electrical speed corresponding to the time derivative of the stator electrical angle. The electrical torque equation of synchronous generator can be written as:

$$P_e = [E'_q + (X_q - X'_d)i_d]i_q - R_s(i_d^2 + i_q^2) \tag{2}$$

By ignoring the damper winding response, the transient response of stator winding and the effect on rotor speed variation, a simplified synchronous generator in Park's framework can be defined as:

$$\begin{cases} T'_{d0}\dot{E}'_q = -E_{fd} - E'_q - (X_d - X'_d)i_d \\ v_d = -R_s i_d + X_q i_q \\ v_q = -R_s i_q - X'_d i_d + E' \end{cases} \tag{3}$$

Where P_e the electromagnetic power of synchronous generator is, E'_q is the transverse electromotive force, X_d and X_q are respectively the direct and transverse resistances, X'_d is the direct transient resistance. The model of PWM rectifier in d-q axis can be described as [11]:

$$\begin{cases} u_{sd} = R_s i_{sd} + \psi_{sd} \cdot d/dt - \omega_r \psi_{sq} \\ u_{sq} = R_s i_{sq} + \psi_{sq} \cdot d/dt + \omega_r \psi_{sd} \end{cases} \tag{4}$$

Where ψ_{sd} and ψ_{sd} are the fluxes and ω_r is the angular speed of the generator shaft.

In order to decouple the d-axis and q-axis components of PWM rectifier, a feedforward decoupling control methed was used [12]. Where $G(s)$ is the transfer function of current regulator, i^*_{sd} and i^*_{sq} is the set values of i_{sd} and i_{sq}. So, the control equation of u_{sd} and u_{sq} is:

$$\begin{cases} u_{sd} = -G(s)(i^*_{sd} - i_{sd}) - \omega_r \psi_{sq} + e_d \\ u_{sq} = -G(s)(i^*_{sq} - i_{sq}) - \omega_r \psi_{sd} + e_q \end{cases} \tag{5}$$

the (5) can be rewritten as:

$$\begin{bmatrix} e_d \\ e_q \end{bmatrix} = \begin{bmatrix} L \cdot d/dt + R_s & \omega_r L \\ \omega_r L & L \cdot d/dt + R_s \end{bmatrix} \begin{bmatrix} i_{sd} \\ i_{sq} \end{bmatrix} + \begin{bmatrix} u_{sd} \\ u_{sq} \end{bmatrix} \tag{6}$$

substitute formula (4) into (6) resulted in:

$$\frac{d}{dt} \cdot \begin{bmatrix} i_{sd} \\ i_{sq} \end{bmatrix} = \begin{bmatrix} i_{sd} \\ i_{sq} \end{bmatrix} \begin{bmatrix} \frac{[G(s) + R_s]}{L} & 0 \\ 0 & \frac{[G(s) + R_s]}{L} \end{bmatrix} - \frac{1}{L} G(s) \begin{bmatrix} i^*_{sd} \\ i^*_{sq} \end{bmatrix} \tag{7}$$

Formula (7) shows that the feedforward decoupling control methed realized the decoupling of i_{sd} and i_{sq}. The measurement unit in PWM rectifier can be equivalent to a small inertial unit $G_m(s) = K_m/(1+\tau_m s)$, combined with PWM rectifier unit, we can get:

$$\frac{dv_f}{dt} = -\frac{v_f}{\tau_m + 3T_s} + \frac{K_{PWM}}{1 + (\tau_m + 3T_s)s} \tag{8}$$

Consider $\dot{v}_f = \frac{R_f}{X_{ad}}\dot{E}_{fd}$ and Substituted into (8) we can get:

$$\dot{E}_{fd} = -\frac{E_{fd}}{\tau_m + 3T_s} + \frac{K_{PWM}X_{ad}}{(\tau_m + 3T_s)R_f}v_c \tag{9}$$

Combined with (3), we can get a 3rd order excitation control model of electrically excited synchronous generator:

$$\begin{cases} \frac{dE'_q}{dt} = \frac{1}{T'_{d0}}E_{fd} - \frac{1}{T'_{d0}}E'_q - \frac{(X_d - X'_d)}{T_{d0}}I_d \\ \frac{dE''_q}{dt} = \frac{c}{T'_{d0}}E_{fd} + (\frac{1}{T''_{d0}} - \frac{c}{T'_{d0}})E'_q - \frac{E''_q}{T''_{d0}} - (\frac{X'_d - X''_d}{T''_{d0}} + \frac{cX'_d - cX''_d}{T'_{d0}})I_d \\ \frac{dE''_d}{dt} = -\frac{1}{T''_{q0}}E''_d + (\frac{X_q - X''_q}{T''_{q0}})I_d \\ \dot{E}_{fd} = -\frac{E_{fd}}{\tau_m + 3T_s} + \frac{K_{PWM}X_{ad}}{(\tau_m + 3T_s)R_f}U_C \end{cases} \tag{10}$$

Where U_C is the output voltage of excitation controller, $c = (X''_d - X_l)/(X'_d - X_l)$.

For the purpose of taking the effect of excitation control on the system stability into account, using the swing equation of synchronous generator in [13]:

$$\begin{cases} \Delta\omega = 1/(2Hs + K_D) \\ \Delta\delta = 2\pi f_0 \Delta\omega / s \end{cases} \tag{13}$$

The torque equation is:

$$\Delta T_e = K_1\Delta\delta + K_2\Delta E'_q \tag{14}$$

And the excitation voltage equation is:

$$(1 + sT'_{d0}K_3)\Delta E'_q = -K_3(\Delta E_f + K_4\Delta\delta) \tag{15}$$

Also the stator voltage equation is:

$$\Delta u_t = K_5\Delta\delta + K_6\Delta E'_q \tag{16}$$

The Low-frequency oscillation matrix equation of synchronous generator for transient stability analysis can be obtained from formula (3), (13), (14), (15) and (16) as is shown in below:

$$\begin{bmatrix} \Delta\dot{\omega} \\ \Delta\dot{\delta} \\ \Delta\dot{E}'_q \\ \Delta\dot{E}_f \end{bmatrix} = \begin{bmatrix} -K_D/2H & -K_1/2H & -K_2/2H & 0 \\ 2\pi f_0 & 0 & 0 & 0 \\ 0 & -K_4/T'_{d0} & -/K_3T'_{d0} & -/T'_{d0} \\ 0 & -K_AK_5/T_A & -K_AK_6/T_A & -/T_A \end{bmatrix} \begin{bmatrix} \Delta\omega \\ \Delta\delta \\ \Delta E'_q \\ \Delta E_f \end{bmatrix} \tag{17}$$

where $K_1 \sim K_6$ represent internal influence factors within the system, which were all described detailly in [13].

3. Design of H_∞ controller

3.1. Design of Excitation Controller

Figure 4 shows the standard H_∞ feedback structure, where r is the system input while y is the output, e is the input error, u is the output of controller, K_{c1} is the controller and P is the general controlled plant. W_1, W_2 and W_3 are respectively the weighting functions of sensitivity function S, input sensitivity function R and penalty sensitivity function T.

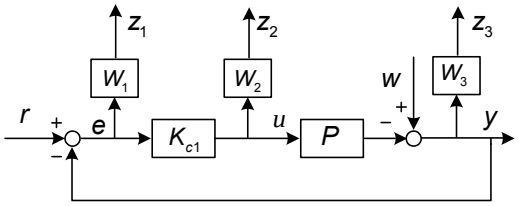

Figure 4. Structure of Standard H_∞ feedback

In the H_∞ control theory, the general controlled plant P is:

$$P = \begin{bmatrix} W_1 & -W_1G \\ 0 & W_2 \\ 0 & W_3G \\ I & -G \end{bmatrix} = \left[\begin{array}{c|cc} A & B_1 & B_2 \\ \hline C_1 & D_{11} & D_{12} \\ C_2 & D_{21} & D_{22} \end{array}\right] \tag{18}$$

And the state space is described as:

$$\begin{cases} \dot{x} = Ax + B_1\omega + B_2u \\ z = C_1x + D_{11}\omega + D_{12}u \\ y = C_2x + D_{21}\omega + D_{22}u \end{cases} \tag{19}$$

Where x is an n-dimensional state variable, ω is an r-dimensional signal vector and u is a p-dimensional control vector. z and y are respectively the expected and measured output. The closed-loop transfer function from w to z can be written as:

$$T_{zw}(s) = LFT(P(s),K(s)) = P_{11} + P_{12}K(I - P_{22}K)^{-1}G_{21}$$

The H_∞ standard problem is to find out wheter there is a controller K with the given H_∞ performance γ to the generalized plant P or not to ensure that the closed-loop system have an internal stability, and $\|T_{z\omega}(s)\|_\infty < 1$ in addition. For the generalized plant shown as formula (18), the H_∞ standard problem based on solving linear matrix inequalities is design a feedback H_∞ controller $u(s) = K(s)y(s)$, which will make the output from w to z is bounded [14].

The inner loop control structure of VRCS uses the stator voltage and field voltage as feedback signals to compare with the set value, and then the H_∞ controller will take the compared error as input signal for field current regulation so as to control the generator output voltage

In the formula (10), let $y = E'_q$, the equation of the electrically excited synchronous containing the excitation system can be written as:

$$\begin{cases} \dot{X} = A_PE + B_{P1}I + B_{P2}U_c \\ y = C_PE \end{cases} \tag{20}$$

Where:

$$X=\begin{bmatrix}E_{fd}\\E'_q\\E''_q\\E''_d\end{bmatrix},\ I=\begin{bmatrix}I_d\\I_q\end{bmatrix},\ A_P=\begin{bmatrix}-1/(\tau_m+3T_s) & 0 & 0 & 0\\ 1/T'_{d0} & -1/T'_{d0} & 0 & 0\\ c/T'_{d0} & 1/T''_{d0}-c/T'_{d0} & -1/T''_{d0} & 0\\ 0 & 0 & 0 & -1/T''_{q0}\end{bmatrix}$$

$$B_{P1}=\begin{bmatrix}0 & 0\\ (X'_d-X_d)/T'_{d0} & 0\\ (X''_d-X'_d)/T''_{d0}+(cX'_d-X_d)/T'_{d0} & 0\\ 0 & (X_q-X''_q)/T''_{q0}\end{bmatrix},\ B_{P2}=\begin{bmatrix}\frac{K_{PWM}(X_d-X_l)}{R_f(\tau_m+3T_s)}\\0\\0\\0\end{bmatrix},\ C_P=\begin{bmatrix}0\\1\\0\\0\end{bmatrix}^T$$

Table 1. Parameters used in Excitation System Model

Labels	Values
Field resistance Rf (pu)	0.0037
d-axis synchronous reactance xd(pu)	1.52
q-axis synchronous reactance xq(pu)	0.996
d-axis transient reactance x´d(pu)	0.152
d-axis subtransient reactance x"d(pu)	0.116
q-axis subtransient reactance x"q(pu)	0.192
d-axis open circuit transient time constant T´d(s)	0.208
d-axis open circuit subtransient time constant T"d(s)	0.022
q-axis open circuit subtransient time constant T"q(s)	0.011
Rotor Inertia H(kgm^2)	109.0223
Equivalent excitation Gain Ka	40
Equivalent excitation time constant Ta (s)	0.1
Generator Inertia time constant H (s)	4.25
Line reactance Xe (pu)	0.5

In this paper, we used the parameters in Table 1 [15] for controller design, the weighting functions W_1, W_2 and W_3 used for H_∞ excitation controller are:

$$W_1=\frac{0.02(s+500)}{s+0.002},\ W_2=1.0\times10^{-5},\ W_3=\frac{0.02(s+10)}{s+80}$$

The controller can be obtained by solving the LMI equation [16]:

$$K_{C1}=\frac{33847993.9183(s+1.561)(s+0.9816)(s+0.7692)}{(s+1.707e005)(s+2.292)(s+1.197)(s+0.03153)}$$

As we can see from above, the zeros and poles of K_{C1} are all in the left half-panel of complex frequency domain, which indicated the closed-loop system is stable.

3.2. Design of PSS

The traditional PSS design method is based on the singular value theory or Glover McFarlane's loop shaping method with defined structure by choosing suitable weighting functions. Usually, the weighting functions used for H_∞ loop shaping method for PSS design is selected by experience trial and error. In this paper, the design of H_∞ PSS was attributed to the mixed sensitivity problem [16], the structure can be seen in Figure 5.

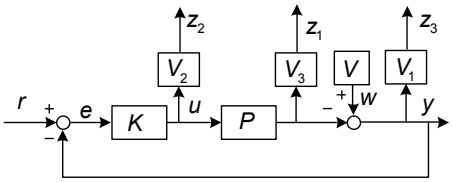

Figure 5. Structure of Mixed Sensitivity Problem

Where $V_1(s)$, $V_2(s)$ and $V_3(s)$ are the weighting functions used for H_∞ PSS design and the weighting function $V(s)$ is used for configuration the poles of system.

In the SMIB system, the PSS designed via H_∞ strategy can be obtained by using $\Delta\omega$ as input and Δu_s for output. Suppose that the sytem variables are $x=[\Delta\omega \quad \Delta\delta \quad \Delta E_q' \quad \Delta E_f]^T$, Δu_E and $\Delta\delta$ are respectively the system input and output, then we can get the output equation and the state equation of the proposed system from (17) as below:

$$\begin{cases} \dot{x} = A_S x + B_S u \\ y = C_S x + D_S u \end{cases} \tag{21}$$

Where:

$$A_S = \begin{bmatrix} -K_D/2H & -K_1/2H & -K_2/2H & 0 \\ 2\pi f_0 & 0 & 0 & 0 \\ 0 & -K_4/T_{d0}' & -/K_3T_{d0}' & 1/T_{d0}' \\ 0 & -K_AK_5/T_A & -K_AK_6/T_A & -/T_A \end{bmatrix} \quad B_S = \begin{bmatrix} 0 \\ 0 \\ 0 \\ K_A/T_A \end{bmatrix} \quad C_S = \begin{bmatrix} 1 \\ 0 \\ 0 \\ 0 \end{bmatrix} \quad D_S=0$$

We can get the characteristic roots: λ_1=-0.0205 $\pm$ j5.3394, λ_2=-17.4215 $\pm$ j50.0488 of A_S by subtituting the parameters in table1. As the weak damping poles (-0.0205 $\pm$ j5.3394) is nearby imaginary axis, the system would instability when a system fault occurs. So we reconfigurated the poles as (-2.22 $\pm$ j5.3394) and obtained V as:

$$V=\frac{(s+2.22+j5.3394)(s+2.22-j5.3394)}{(s+0.0205+j5.3394)(s+0.0205-j5.3394)}=\frac{s^2+4.44s+33.438}{s^2+0.053s+28.51}$$

weighting functions $V_1(s)$ and $V_3(s)$ are respectively:

V_1=0.3(s + 50)/(s+4), V_3=(s+6)/(s+880)

As the frequency of low-frequency oscillation in power system ranges from 0.7 to 2Hz, we can get:

$$V_2(s)=\frac{0.0002s+0.01}{0.5s+1}$$

an 18 order H_∞ controller can be obtained by solving Riccati equation [17], in order to have an easily realization, a 3rd order H_∞ controller with stable zeros and poles was get by order deduction.

$$K_{C2}=\frac{-624.6s^2-8.978s-17860}{s^3+12.46s^2+28.62s+355.6}$$

4. Simulation Analysis

Figure 6(a) and Figure 6(b) are respectively the rotor speed and stator voltage of EESG with a 0.04 pu fluctuation of mechanical power sustained for 100 milliseconds at 3.0 seconds. What we can see from figure is that the rotor speed and the stator voltage would pass into a stable level quickly with single H_∞ excitation control, but the amplitude of adjustment process was greater and the oscillation time was longer than which used both H_∞ excitation control and H_∞ PSS. This indicated that the double H_∞ control was more effective to ensure that the system can remain at a stable level.

With a 20% and a 40% input mechanical power reduction, the active power of FSCWT can be seen in Figure 7(a) and Figure 7(b), the stator voltage can also be seen in Figure 7(c) and Figure 7(d) and the reactive power were shown in Figure 7(e) and Figure 7(f) respectively. What we can see from figure is that the stator voltage can remain at a stable in short times as the input mechanical power of generator reduced. What's more, the stator voltage and reactive power of FSCWT with double H_∞ control is of a better stability performence than which used only H_∞ excitation control.

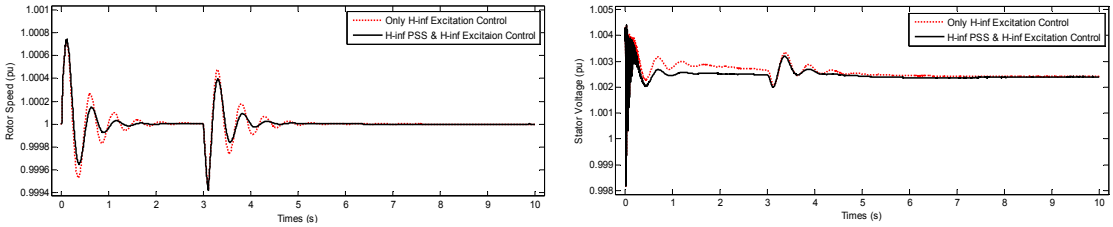

(a) Rotor speed of EESG (b) Stator voltage of EESG

Figure 6. Response of EESG with a Mechanical Power Fluctuation

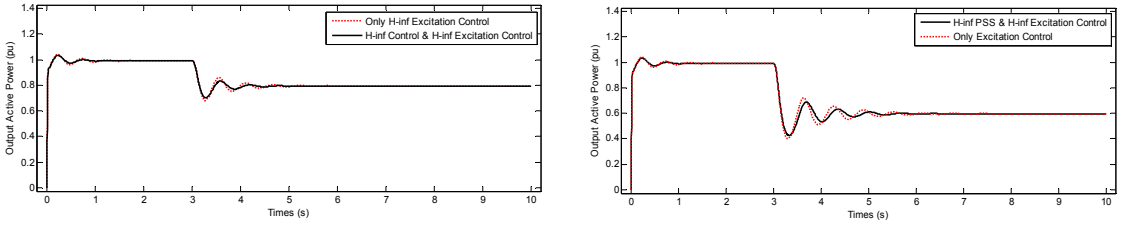

(a) Active power of EESG with a 20% Pm reduction

(b) Active power of EESG with a 40% Pm reduction

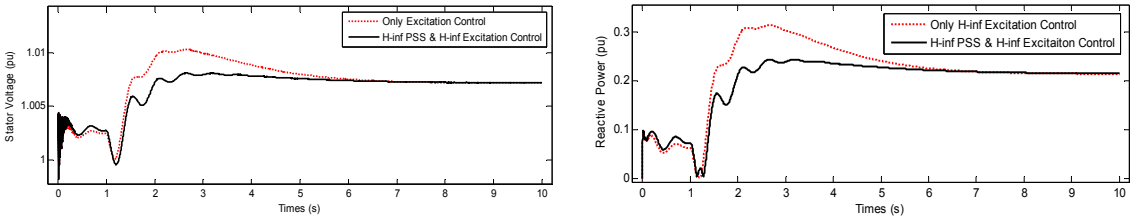

(c) Stator voltage of EESG with a 20% Pm reduction

(d) Reactive power of EESG with a 40% Pm reduction

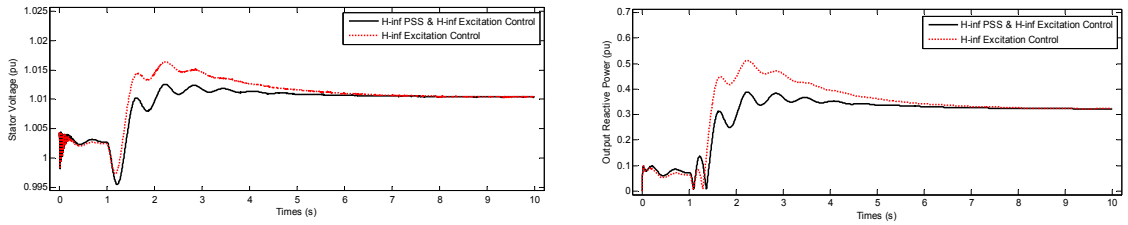

(e) Stator voltage of EESG with a 20% Pm reduction

(f) Reactive power of EESG with a 40% Pm reduction

Figure 7. Voltage and Reactive Power of EESG with a Reduction of Pm

In order to verify the transient performance of VRCS with a H_∞ PSS, a three phase fault was set at 1.0s with 120ms lasted. As we can see in Figure 8(a) and Figure 8(b), the excitation systems responsed as quickly as the short occured to produce reactive power so as to maintain the stator voltage at a stable level. When the fault is cleared, the stator voltage and rotor speed can remain to the original value in a short time as is shown in Figure 8(c) and Figure 8(d). Compared with the single H_∞ excitation control, the double loop control with H_∞ exciter and H_∞ PSS not only realized fast excitation but also achieved transient stability of the proposed system.

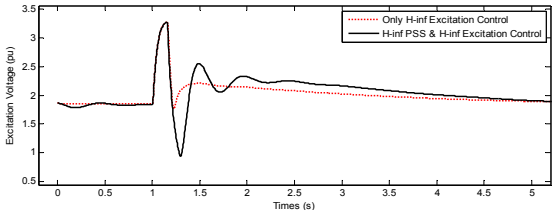

(a) Field voltage of EESG with a 3-phase short

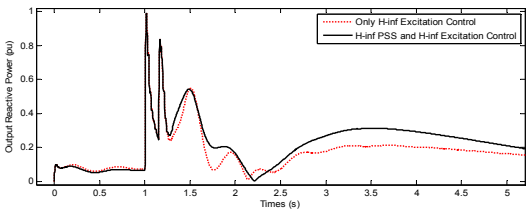

(b) Reactive power of EESG with a 3-phase short

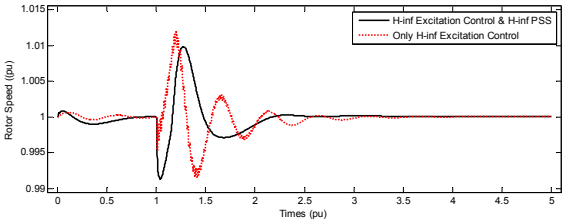

(c) Rotor speed of EESG with a 3-phase short

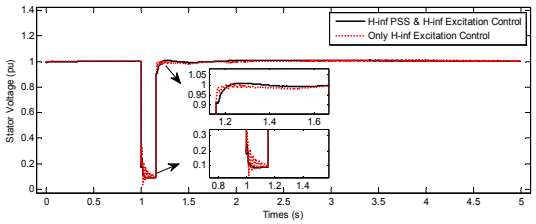

(d) Stator voltage of EESG with a 3-phase short

Figure 8. Transient Response of EESG with H_∞ PSS and H_∞ excitation Controller

5. Conclusion

A stable output reactive power and voltage of FSCWT has an important influence on the stability of power system with large-scale wind farms connected to the grid. The excitation system parameters will change as the operation condition changes and an approximation of the system model causes the uncertainty of the actual controlled plant model, which results in an undesirable control effect of the VRCS in a wide range. The exciter and PSS based on H_∞ control theory collected the uncertainty and nonlinear into design, which is of a good robustness and radically improves the system stability. The VRCS used in this paper enabled the EESG with a fast excitation, which brought negative damping at the same time. What is gratifying is that the VRCS also taken the influence of fast excitation on transient stability in accout on the bases of voltage feedback control. Simulation results show that the VRCS has a strong robustness, which embodies the effectness of double H_∞ control in fast excitation system to realize the voltage and reactive power control.

Acknowledgement

This paper was funded by the National 863 project: Design and Manufacturing Technology of Front-end Speed Controlled Wind Turbines (2012AA052901).

References

[1] Simon De Rijcke, Hakan Ergun. Grid Impact of Voltage Control and Reactive Power Support by Wind Turbines Equipped With Direct-Drive Synchronous Machines. *IEEE Transactions on Sustainable Energy*. 2012; 3(4): 890-898.
[2] YANG Bai-jie, CHAO Qin, YUAN Tie-jiang, YI Hai-dong. Research of STATCOM Impact on Wind Farm LVRT and Protection. *TELKOMNIKA Indonesian Journal of Electrical Engineering*. 2012; 10(8): 2117-2124.
[3] Balduino Cezar Rabelo, Wilfried Hofmann. Reactive Power Control Design in Doubly Fed Induction Generators for Wind Turbines. *IEEE Transactions on Industrial Electronics*. 2009; 56(10): 4154-4162.
[4] Andreas Besteck. *WinDrive-variable Speed Wind Turbines without Converter with Synchronous Generator*. 2009.
[5] Emile Mouni, Slim Tanai. Synchronous Generator Output Voltage Real-Time Feedback Control via H∞ Strategy. *IEEE Trans. on Energy Conversion*. 2009; 24(2): 329-337.

[6] Balduino Rabelo, Wilfried Hofmann. *Voltage Regulation for Reactive Power Control on Synchronous Generators in Wind Energy Power Plants*. Nordic Workshop on Power and Industrial Electronics (NORPIE). Norway. 2004: 1-6.
[7] Abraham Lomi, Dhadbanjan Thukaram. Optimum Reactive Power Dispatch for Alleviation of Voltage Deviations. *TELKOMNIKA Indonesian Journal of Electrical Engineering*. 2012; 10(2): 257-264.
[8] IEEE Standards Board. 421.5-1992. *IEEE Recommended Practice for Excitation System Models for Power System Stability Studies*. New York: IEEE Press; 1992.
[9] Uwe Reimesch. *A Converterless Drive Train Concept for Grid Friendly Wind Turbines*. GM Sales of Voith Turbo Wind. 2010.
[10] Emile Mouni, Slim Tanai. *Synchronous Generator Output Voltage Control via A Generalized Predictive R S T Controller*. IEEE International Symposium on Industrial Electronics. Cambridge. 2008: 718-723.
[11] Sebastian Rosado, Xiangfei Ma. Model-Based Digital Generator Control Unit for a Variable Frequency Synchronous Generator with Brushless Exciter. *IEEE Transactions on Energy Conversion*.2008; 23(1): 42-52.
[12] Marian P. Kazmierkowski, Luigi Malesani. Current Control Techniques for Three phase Voltage-source PWM Converters: A Survey. *IEEE Transactions on Industry Electronics*. 1998; 45(5): 691-703.
[13] Göran Andersson. Dynamic and Control of Electric Power System. ETH Zürich: 2012.
[14] Kemin Zhou, John C. Doyle. Essentials of Robust Control. Prentice Hall. 1st Edition. New Jersey: 1997.
[15] Markus Poller. *Grid Compatibility of Wind Generators with Hydro-dynamically Controlled Gearbox with German Grid Codes*. Voith Turbo Wind GmbH & Co. KG. 2008.
[16] Chuanjiang Zhu, Mustafa Khammash. Robust Power System Stabilizer Design Using H_∞ Loop Shaping Approach. *IEEE Transactions on Power Systems*. 2003; 18(2): 810-818.
[17] A Barakat, S Tnani. Output Voltage Control of Synchronous Generator Using Diode and Thyristor Excitation Structures Combined with Multivariable H_∞ Controllers. *IET Electric Power Applications*. 2012; 6(4): 203-213.